

Calibration of the NASA Scatterometer using a ground calibration station

Richard D. West, Wu-Yang Tsai, James L. Granger, and William H. Daffer

Jet Propulsion Lab
California Institute of Technology
4800 Oak Grove Dr.
Pasadena CA 91109-8099 USA

ABSTRACT

To aid in calibrating and monitoring the performance of the NASA scatterometer (NSCAT), a calibration ground station (CGS) was operated in White Sands, New Mexico from mid November 1996 through February 1997. The CGS was used to verify the proper operation of the NSCAT system including transmit power, frequency, pulse width, and receiver gain. It was also used to track spacecraft attitude variation, and to measure the antenna gain balance between different beams. This paper will describe the basic operation of the CGS, and the principle results obtained during the calibration period. The CGS is a transmit/receive system which was used to record pulses from NSCAT, and to transmit pulses back to NSCAT. The CGS data was synchronized with NSCAT telemetry, and processed for timing, frequency, and gain information. These results were then compared with the values expected using the nominal pre-launch calibration data. Timing discrepancies indicated significant spacecraft attitude variations beyond the values reported in telemetry. Gain discrepancies showed a small ascending/descending difference. The cause of this difference (NSCAT or the CGS) is not clear at this time.

Keywords: NSCAT, scatterometer, radar, calibration

1. INTRODUCTION

The NASA Scatterometer (NSCAT) operated from August 1996 through June 1997 on the Japanese Advanced Earth Observation Satellite (ADEOS). The primary mission of NSCAT was to measure ocean surface vector winds by accurately measuring the backscattering cross-section at Ku band.¹ The backscattering cross-section is related to the wind induced surface roughness. NSCAT also provided useful data over land and ice with many important applications in remote sensing.

To aid in calibrating and monitoring the performance of NSCAT, a calibration ground station (CGS) was operated in White Sands, New Mexico from mid November 1996 through February 1997. The CGS was used to verify the proper operation of the NSCAT system including transmit power, frequency, pulse width, and receiver gain. The timing of the observations allowed the CGS to track the spacecraft attitude under certain assumptions described later. The CGS received powers were used to measure the antenna gain balance between the different beams. This paper describes the operation of the CGS, and the principle timing and gain results obtained during the calibration period.

Section 2 describes the operation of the CGS and the data obtained. Section 3 discusses the timing analysis performed on the data. Section 4 uses the timing results to determine spacecraft attitude variation, and section 5 looks at the analysis of antenna gain relative balancing.

2. CGS OPERATION

The CGS consists of a Ku band transmitter and corresponding receiver. Both use the same antenna, and are automatically controlled by a dedicated computer system. Several minutes before ADEOS is due to fly by, the CGS slews to the predicted azimuth and elevation at which the first NSCAT beam should appear, and begins "listening" for the NSCAT transmissions. NSCAT transmits a set of 25 pulses, and then receives for four pulse periods. As soon as the CGS detects this characteristic pattern, it begins recording the NSCAT pulse data, and transmitting synchronized bursts of broadband noise when NSCAT is in receive only mode. The CGS receiver mixes down the NSCAT transmissions by 13.995 GHz, leaving the signal with just the doppler frequency due to the relative motion

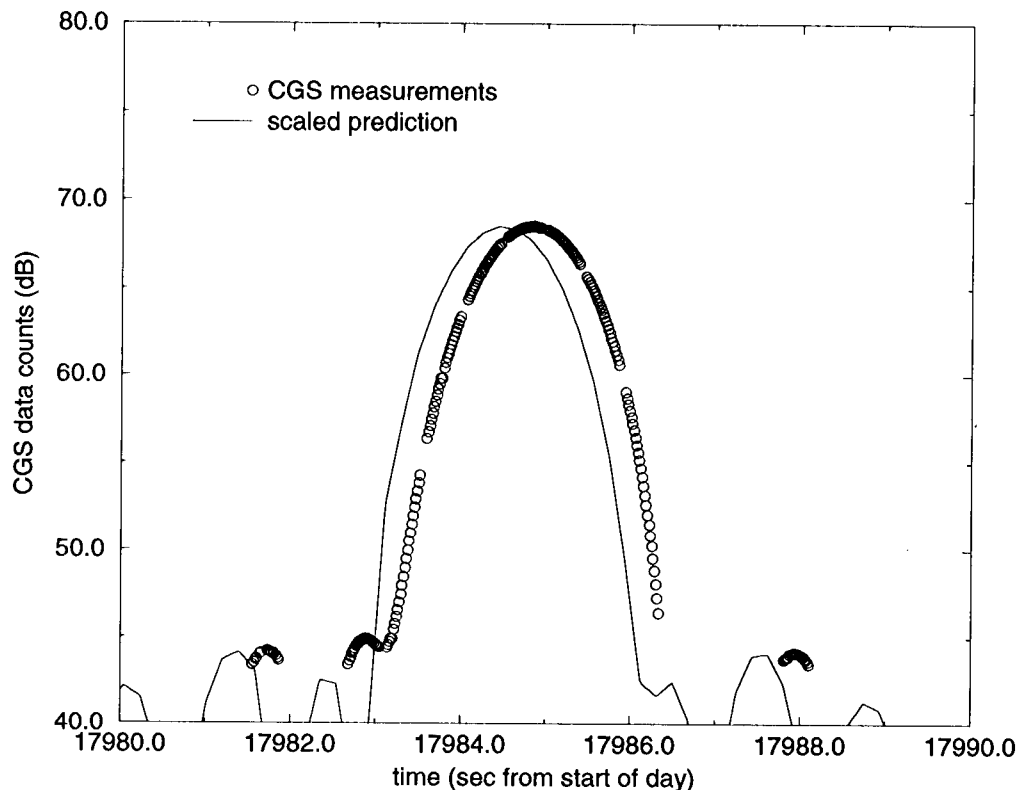


Figure 1. Example beam crossing for the left side midbeam (ie., 5V). Circles are the CGS power measurements while the solid line gives the predicted power computed from the geometry and pre-launch antenna patterns. The vertical scale is raw CGS data counts converted to dB. The predicted power is scaled to match the peak of the first beam crossing (6V) to be consistent with the beam balance definition used in fig. 7

of the spacecraft with respect to the CGS. Doppler frequencies range from 35 KHz to 220 KHz for the CGS data passes; positive for the forward looking beams and negative for the backward looking beams. The mixed down signal is sampled at 1.6 MHz, and stored in memory for later transfer.

To aid in providing complete coverage of the antenna pattern, NSCAT is commanded to pulse continuously on the beam passing over the CGS. The NSCAT beam sequence commanding and the associated CGS slew commanding are based on predicted ephemeris data, and orbit propagation.

Fig. 1 shows the CGS measurements from a representative ascending beam crossing on Jan 3, 1997. Three peaks like this are swept out by the three NSCAT beams on one side. The vertical scale is in raw data counts which is proportional to received power (converted to dB). The 25 pulse sequences separated by 4 pulse period gaps are readily apparent, and the peak of the NSCAT antenna pattern is easily obtained. In the next sections, we describe how this data set can be used to diagnose problems, and help in calibrating the antenna patterns.

3. TIMING ANALYSIS

Perhaps the simplest way to use the CGS data is to look at the timing of the received powers. In particular, the observed time of the peak power can be compared with the expected time of the peak power as shown in fig. 2. The difference between these two times can potentially provide us with important information about NSCAT and

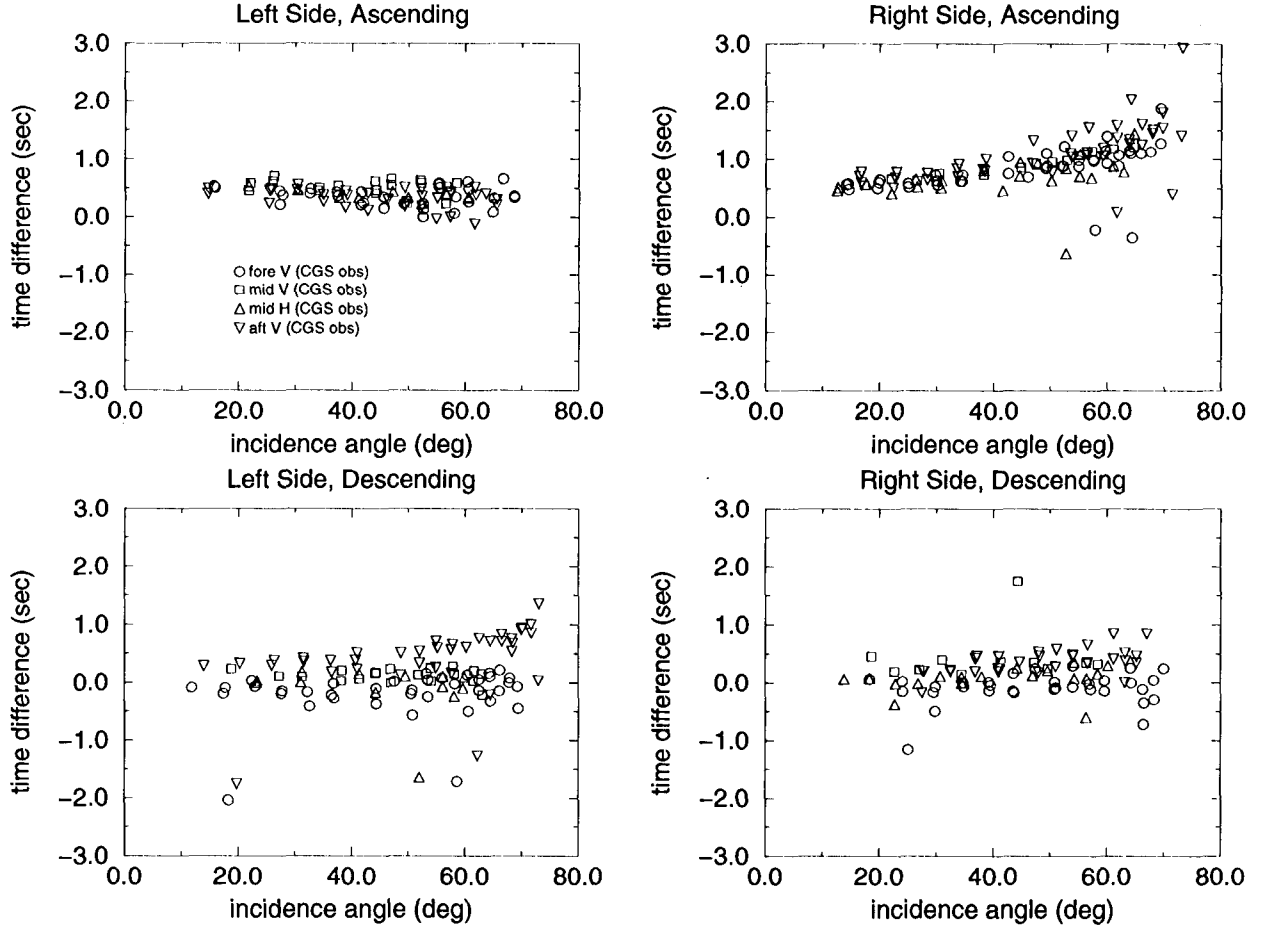


Figure 2. Timing errors as a function of incidence angle (at the CGS) separated by which side of the nadir track the CGS was located, and by ascending or descending passes by ADEOS. The time error is defined to be the observed beam crossing time minus the predicted beam crossing time.

ADEOS. The time difference is affected by the attitude of the spacecraft, the attitude of the NSCAT antenna relative to the spacecraft, the accuracy of the spacecraft ephemeris, the accuracies of the spacecraft and CGS clocks, and the synchronization error between the two clocks (shown in fig. 3). Before we discuss these possible causes of the time difference, we will first examine how the two times are determined.

3.1. Observed Peak Power Time

The CGS provides a time tag for each pulse measurement. The time tag comes from a GPS receiver, and is recorded at the end of each pulse. The analysis software subtracts half the pulse width (2.5 msec) from each time tag to put them at the center of the pulse. The GPS time is very accurate (μsec accuracy), but the peak power location procedure introduces a greater algorithmic uncertainty in the observed peak power time.

One way to determine the observed peak time is to simply pick out the time of the “highest” received power. This approach is somewhat inaccurate because the CGS received powers often contained some small variation near the peak that make the “highest” pulse power difficult to identify. Occasional spurious high measurements also need to be filtered out before picking the highest pulse power. Since the observed powers are expected to vary smoothly along a curve determined mostly by the NSCAT antenna gain variation, we can improve the accuracy of the peak time (and level) by fitting a smooth curve through the points comprising the main lobe. We fit a fourth order polynomial in the least squares sense to the main lobe data. The main lobe data is defined to be all the measurements with

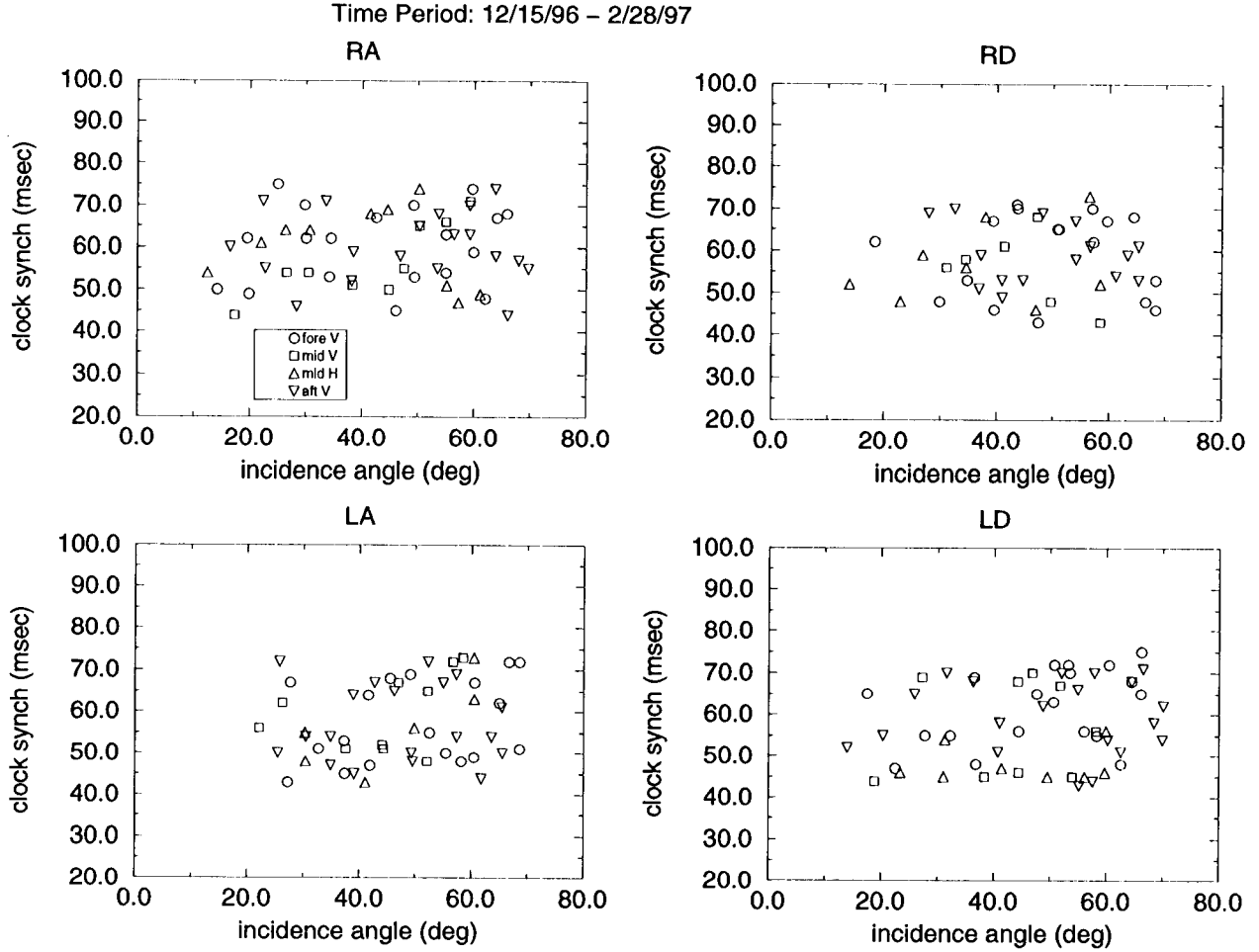


Figure 3. Clock synchronization difference as a function of incidence angle (at the CGS) and separated according to which side of the nadir track the CGS was located, and by ascending or descending passes by ADEOS. The clock synchronization is defined to be the CGS frame time minus the corresponding NSCAT frame time.

power greater than one half the power level of the highest non-glitch measurement. The peak of the fitted polynomial is then determined with a precision of 1 msec.

3.2. Predicted Peak Power Time

The expected or predicted hit time is determined using NSCAT/ADEOS telemetry, the position of the CGS, and prelaunch antenna pattern measurements for the NSCAT antenna and the CGS antenna. No CGS power measurements are used. The power that the CGS should measure is computed from the prevailing geometry as a function of time, and the measured antenna patterns. The governing equation is the one-way radar equation,

$$P_{R_{CGS}} = P_{TPM} e_{st} e_{wt} G_a \frac{\tau}{4\pi r^2} \frac{G_{cgs} \lambda^2}{4\pi} + P_n. \quad (1)$$

In this equation, $P_{R_{CGS}}$ is the predicted power that should be received by the CGS, P_{TPM} is the measurement from the NSCAT transmit power meter, e_{st} and e_{wt} are the transmission efficiencies of the NSCAT switching matrix and waveguides respectively, G_a is the NSCAT antenna gain, τ is the transmissivity of the atmosphere along the look direction, r is the slant range along the look direction, G_{cgs} is the CGS receiving antenna gain, λ is the operating wavelength of the NSCAT transmitter, and P_n is the thermal noise level in the CGS receiving system.

For the purpose of timing and attitude analysis, we assume that all of the terms on the right side of the equation above are constant for the duration of a beam cut (a few seconds) except G_a , G_{cgs} , and r . The values of G_a and

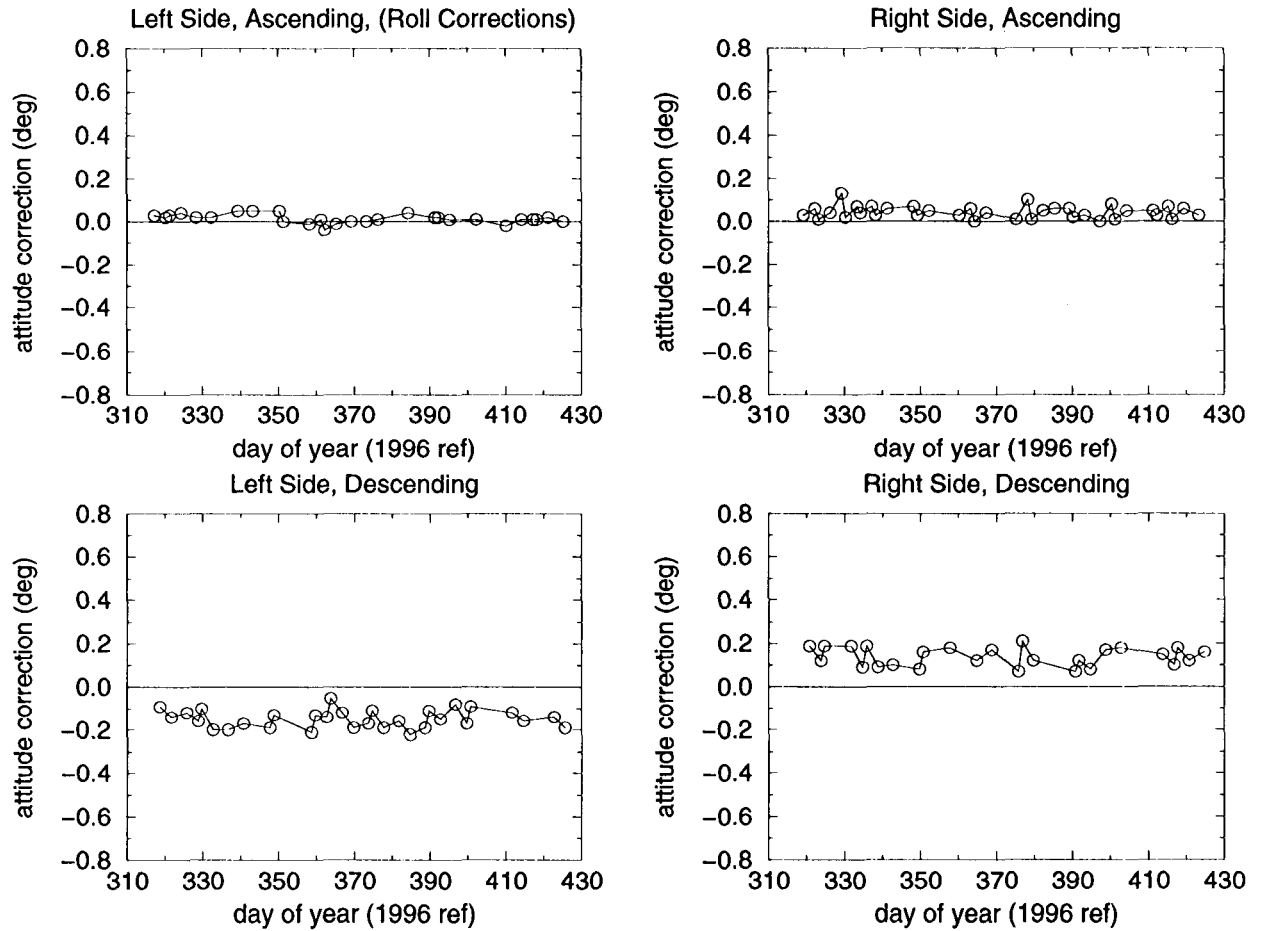


Figure 4. Roll corrections (additive) computed from timing errors and plotted as a function of time; separated by which side of the spacecraft the CGS was on and by ascending or descending pass.

G_{cgs} are both interpolated from prelaunch pattern measurements for the antenna look directions determined by the prevailing geometry. The prevailing geometry is determined using the spacecraft position (from the ephemeris), the spacecraft attitude (from ADEOS telemetry), the NSCAT antenna deployment angles (nominal prelaunch values), the CGS position (measured by GPS), and the commanded CGS pointing. As ADEOS orbits past the CGS, the NSCAT gain pattern sweeps over the position of the CGS, making the predicted power rise and fall. In fig. 1, the predicted CGS power is plotted as a solid line. The noise power P_n is left out because the CGS beam crossing measurements typically have a SNR of 30 dB or higher.

The time of the predicted peak power should match the time of the observed peak power if the geometry information is correct. The level of the predicted peak power will be different from the observed peak power level because the CGS data is not calibrated against an absolute reference. In fig. 1 the predicted power is scaled to match the peak level of the first beam crossing (6V). Mispointing of the CGS antenna could cause some time error in principle, because the CGS antenna gain might vary out of step with the NSCAT antenna gain. In practise, however, the CGS antenna pattern is much broader than the NSCAT gain patterns, so the NSCAT antenna gain variation dominates the predicted power variation.

The NSCAT antenna gain pattern was sampled at NIST with 0.06 deg. spacing in the narrow beam direction and 0.5 deg. spacing in the broad beam direction. The discrete sampling introduces an uncertainty in locating the peak time. Since we expect the antenna gain pattern to vary smoothly over the peak, we again fit a fourth order polynomial to the main lobe points and determine the peak time with a precision of 1 msec.

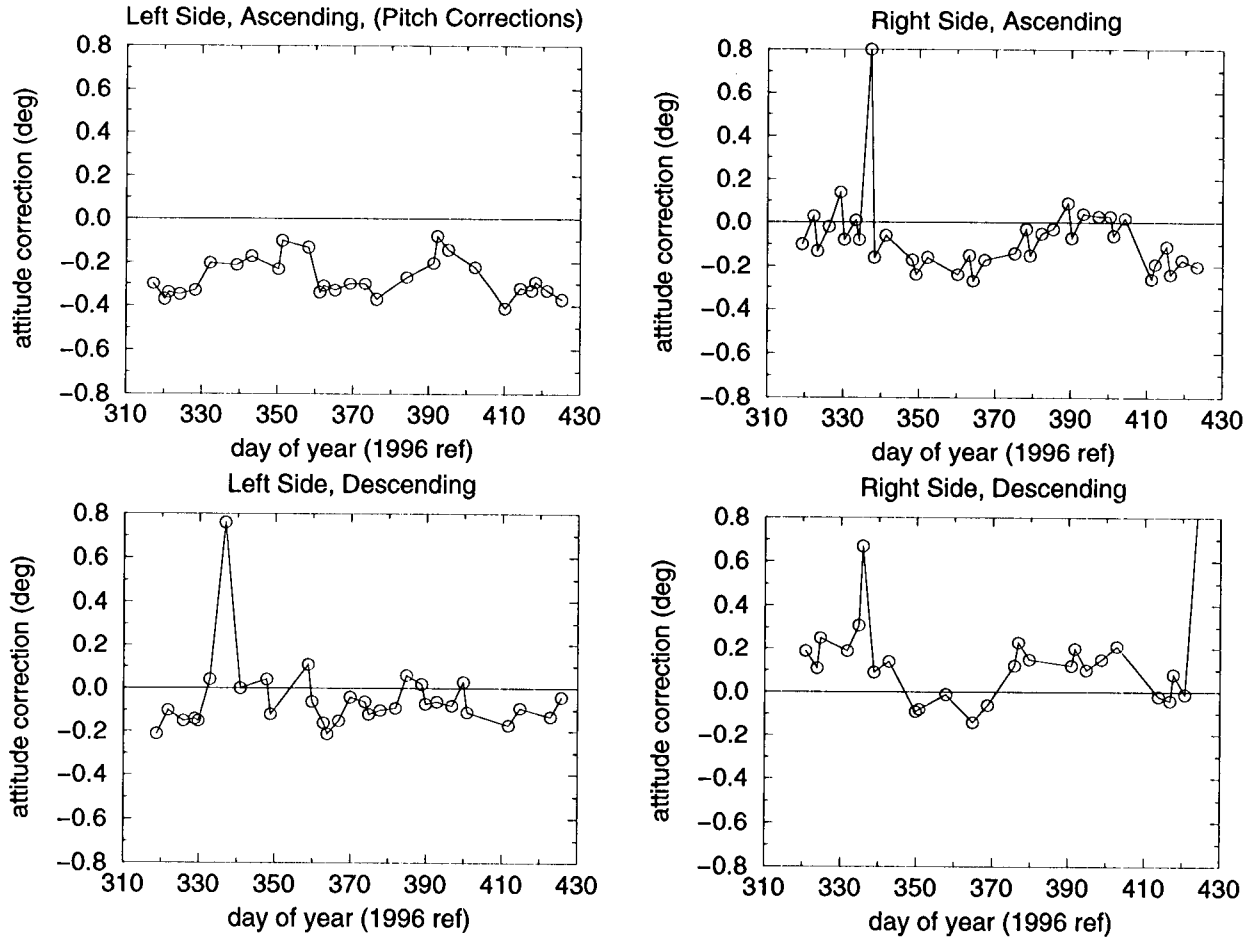


Figure 5. Pitch corrections (additive) computed from timing errors and plotted as a function of time; separated by which side of the spacecraft the CGS was on and by ascending or descending pass.

3.3. Timing Errors - Results and Possible Causes

We define the timing error to be the difference between the observed peak power time and the nominal predicted peak power time,

$$\delta t = t_{\text{obs}} - t_{\text{pred}}. \quad (2)$$

Thus, a positive timing error means that the peak power arrived later than expected. Fig. 2 shows the timing errors for all of the CGS passes as a function of incidence angle (at the CGS). These figures show time differences ranging from a few tenths of a second up to two seconds. To understand these differences and the accuracy of the time measurements, we now look at different possible causes of timing errors.

3.3.1. Observed Peak Time - Accuracy Issues

Error in the observed peak time is dominated by the difference between the GPS derived CGS clock time, and the NSCAT instrument time. The two clocks are synchronized by looking for the CGS transmit pulses in the NSCAT received powers. The NSCAT received powers provide a distinctive signature which allows the NSCAT frames to be associated with the corresponding set of 25 CGS received pulse powers. There is, however, an unavoidable uncertainty due to the 32 Hz granularity of the ADEOS and NSCAT clocks. The uncertainty equals one clock tick or 31.3 msec. Fig. 3 shows the difference computed between the two clocks after synchronizing the frames with the CGS transmissions. As expected, the difference has a uniformly distributed uncertainty of about 32 msec, with no apparent dependence on incidence angle or the circumstances of a data pass (ascending/descending, right/left). It

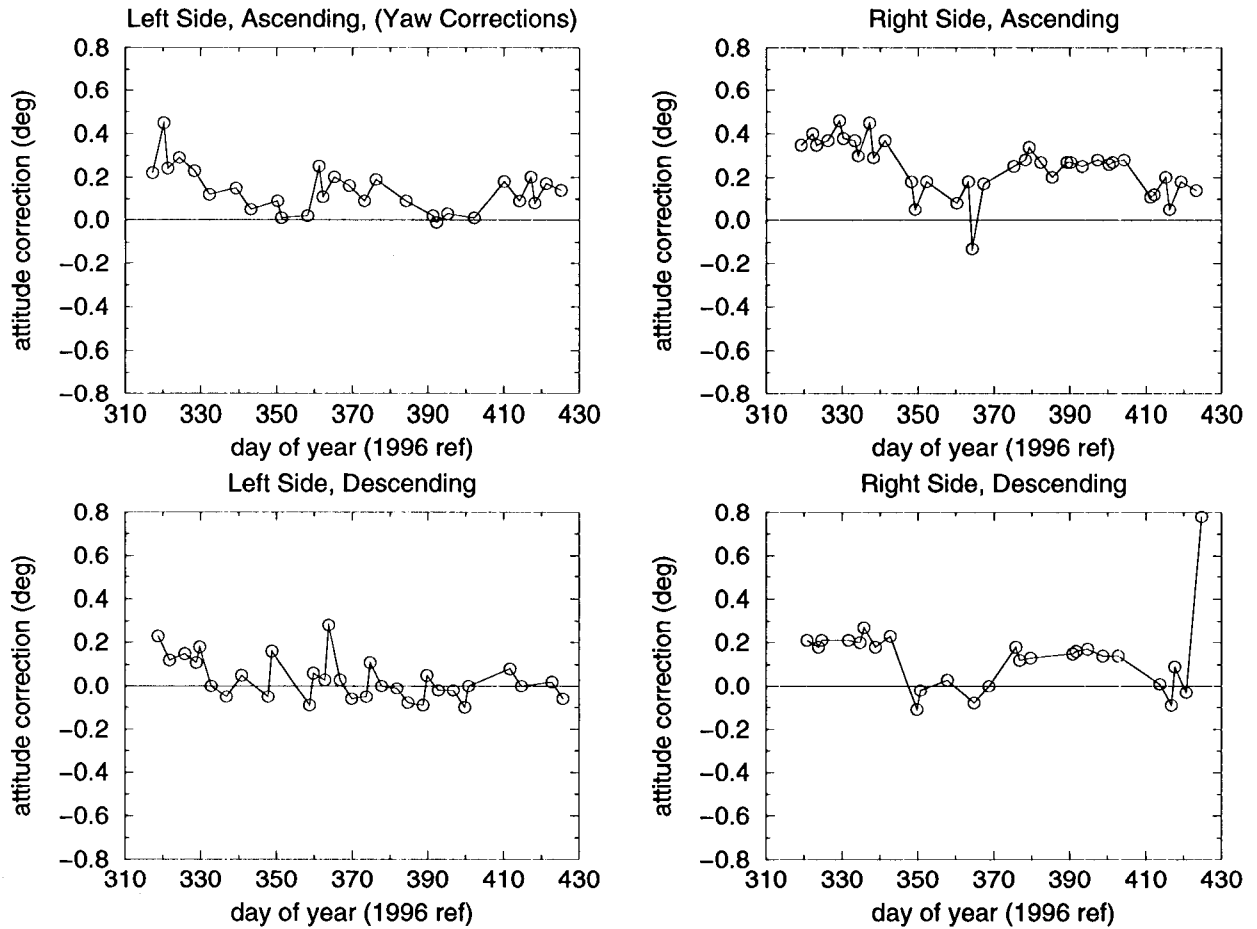


Figure 6. Yaw corrections (additive) computed from timing errors and plotted as a function of time; separated by which side of the spacecraft the CGS was on and by ascending or descending pass.

also has an average level of about 60 msec which comes from a small offset between the NSCAT clock and GPS time. This offset is subtracted out before any further processing.

3.3.2. Predicted Peak Time - Accuracy Issues

The accuracy of the predicted peak time is determined by how well we know the prevailing geometry and the accuracy of the relevant antenna boresight direction. The prevailing geometry is determined by spacecraft position (from the predicted ephemeris), spacecraft attitude (which uses spacecraft velocity as part of the definition), antenna attitude (deployment accuracy), and the CGS position (from GPS).

The determined ephemeris is supposed to be accurate to 100 meters. Our analysis uses the predicted ephemeris available when the CGS data was collected. The predicted ephemeris differs from the determined ephemeris by about 100 meters on the average. Thus, the predicted ephemeris should have an average error of about 200 meters, which corresponds to a time error of about 30 msec.

Errors in the reported spacecraft attitude lead to timing errors by deflecting the boresight along track away from the predicted location. The deflection can be estimated using simple geometry and some typical numbers. The ADEOS spacecraft was supposed to report its attitude to within 0.05 deg (1σ). The ground track velocity is about 6.5 km/s, and the range from the spacecraft to the ground target varies from 850 km to 1800 km. For an angular deflection of 0.05 deg (assumed to be along track), we get a time error ranging from 0.11 to 0.24 seconds. In practise, the deflection will not always be purely along track, so the typical values should be smaller.

4. SPACECRAFT ATTITUDE FROM TIME DIFFERENCES

The observed timing errors are much larger than would be expected based on the uncertainties in the observed and predicted beam crossing times. From this we infer that some aspect of the predicted geometry is less accurate than expected. The increase in timing errors with increasing incidence angle suggests that the spacecraft attitude is at fault.

The timing errors from three separate beam crossings in one data pass can provide information about the spacecraft attitude if certain assumptions are made. Most importantly, the antenna deployment attitude must be assumed to be correct, or at least known. Otherwise, there is not enough information to separate the effects of spacecraft attitude variations from antenna deployment variations. Even if the antenna deployment angles are assumed to be off by fixed values over many data passes, it is still not possible to separate these biases from spacecraft attitude variations. With these concerns in mind, Figs. 4, 5, and 6 show the spacecraft attitude corrections that are required to zero out the timing differences when the nominal antenna deployment angles are assumed to be correct.

The combined timing error uncertainty of about 42 msec translates to fitted attitude uncertainties of 0.02, 0.08, and 0.15 degrees for roll, pitch, and yaw respectively (worst case or 3σ values). These attitude corrections are applied to the reported spacecraft attitude before proceeding to the beam balance analysis.

Figs. 4 – 6 show some substantial attitude variations that were initially quite surprising. Attitude variations by ADEOS of this magnitude were confirmed by separate analysis of NSCAT σ_0 data,² and by an attitude study performed at the Goddard Space Flight Center.³ The particularly large pitch corrections which occur around day of year 335, however, are most likely caused by ephemeris errors which also can cause timing discrepancies. The ephemeris error is inferred because these points show a large doppler error not found elsewhere in the CGS data. We also see some differences between ascending and descending passes, and between right and left side passes. The ascending/descending differences may be explained by day/night differences in the ADEOS attitude control system, or by thermal flexing of the NSCAT antenna. It seems unlikely that the right/left differences are due to ADEOS attitude variation because there is no plausible mechanism that lets the spacecraft “know” which side of the CGS it is passing by. Instead, the right/left differences are probably due to small NSCAT antenna deployment angle biases away from the nominal values measured pre-launch.

5. ANTENNA GAIN BALANCE

One of the goals of the CGS operation was to provide a relative gain balance between the eight NSCAT beams. Well balanced beams are particularly important for wind observations because the wind direction is derived from the small differences between σ_0 observations taken at different azimuth angles. To minimize stability issues, we will look at beam balances for each side of the spacecraft separately. Assuming that the CGS receiver gain is stable during each data take, we can balance the beams after correcting for differences caused by the different geometries during each beam crossing. The procedure starts by calculating the absolute gain error for each beam peak gain. Referring again to fig. 1 and eqn. (1), we solve for the NSCAT antenna gain (G_a) and obtain a similar pair of curves for the observed and predicted antenna gain. The observed antenna gain is off by an absolute calibration factor, but this is not important because we are interested in the differences between the absolute gain errors, not the values themselves. The absolute error is the ratio of the observed peak gain to the predicted peak gain (both located as described earlier). In practise, we also apply the attitude correction described earlier, therefore the predicted peaks will line up in time with the observed peaks. The levels also shift a small amount, but the attitude correction tends to shift the level of all three predicted peaks by the same amount, so it is not a big concern for beam balancing. Once the absolute gain errors are determined, we ratio a reference beam with all three beams to determine the beam balances. Thus, the beam balance for beam 1V is the amount of gain (in dB) which needs to be added to the 1V antenna pattern to give it the same absolute error as the 3V pattern. The correction is applied at the antenna angle corresponding to the CGS measurement. In fig. 1, the predicted peak is 0.17 dB higher than the measured peak, thus the beam balance is -0.17 dB indicating that the NSCAT antenna gain needs to be reduced by that much to make the predicted peak match the observed peak.

Fig. 7 shows the relative antenna gain balances obtained for all the beams. The right side beams are referenced to 3V, while the left side beams are referenced to 6V. The choice of references is arbitrary; these choices provide the cleanest set of gain balances. The data are plotted against incidence angle which relates directly to the broad beam location. Two different symbol types are used to distinguish data taken from ascending passes and from descending passes. Data before day of year 350 (Dec. 15, 1996) are not included in the beam balancing because of problems

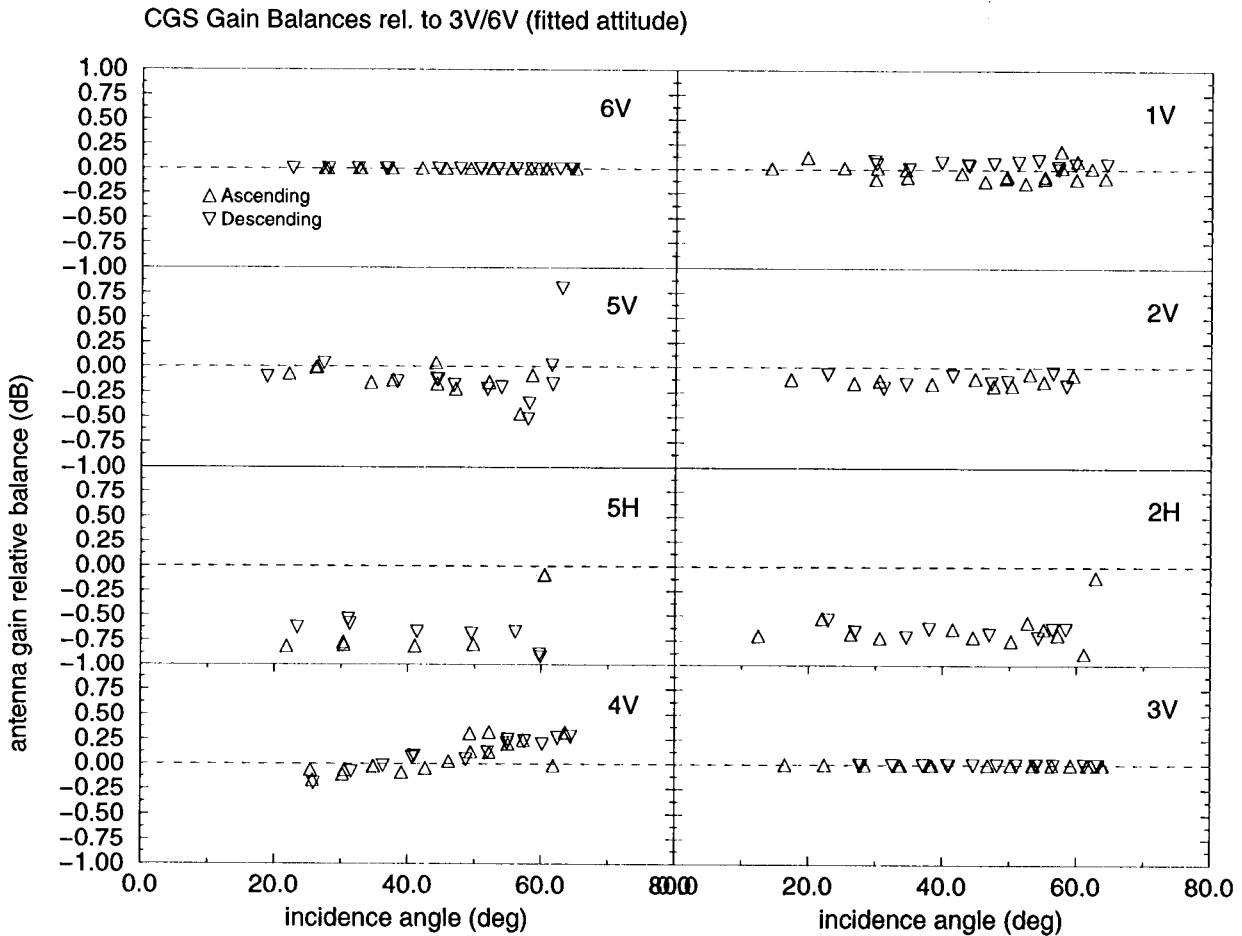


Figure 7. Relative antenna gain balances as a function of incidence angle (at the CGS). Upward triangles are data from ascending passes, downward triangles are data from descending passes. Computed from CGS data corrected with the preceeding attitude fits

with the CGS operation, and because of other confounding effects (eg., orbit maneuvers leading to ephemeris errors). Data beyond 65 deg. incidence angle are also excluded because of possible multipath effects, and higher atmospheric losses.

Most of the beam balance results are quite small, but some surprising features are present. The H-pol midbeams seem to need a fairly large adjustment of about -0.6 dB relative to the V-pol beams. There also seems to be a small difference between the ascending/descending beam balances for 1V, 5H, and 4V. In principle, there should be no distinction between ascending and descending passes, however, the thermal environment on the spacecraft and at the CGS are different because ascending passes always occur at night, while descending passes occur in daylight. It is unclear at this time whether the ascending/descending difference is due to CGS gain variations or NSCAT gain variations. Ascending vs descending beam balance differences of a few tenths of a dB were also obtained in a separate distributed target analysis applied to NSCAT σ_0 data,² however, the overall level of these beam balances are quite different from the CGS beam balances. The causes of these differences are still unknown.

6. CONCLUSIONS

The preceeding analysis demonstrates some of the diagnostic and calibration functions that a ground calibration station can provide for microwave sensors. Both spacecraft and instrument problems can be detected by analyzing time, frequency, and power data from a ground receiver. For NSCAT on ADEOS, timing discrepancies from the

CGS indicates significant attitude variation beyond the values reported in telemetry. Beam balance adjustments from CGS power measurements show a small ascending/descending difference (about 0.2 dB) for some of the beams, however, the cause of this difference is not known.

ACKNOWLEDGMENTS

This work was performed under contract with the National Aeronautics and Space Administration at the Jet Propulsion Laboratory, California Institute of Technology.

REFERENCES

1. F. M. Naderi, M. H. Freilich, and D. G. Long, "Spaceborne radar measurement of wind velocity over the ocean - an overview of the NSCAT scatterometer system", *Proceedings of the IEEE* **79**, pp. 850-866, 1991.
2. W. Tsai et. al., "Post-launch sensor verification and calibration of the NASA scatterometer", submitted to *Trans. on Geoscience and Remote Sensing - ADEOS mission special issue*, June, 1998.
3. R. Luquette, J. Hashmall, J. Landis, and J. Sedlak, "ADEOS attitude determination and analysis - Final Report", available from the Goddard Space Flight Center, Jan. 31, 1998.